

Study on functionalizing the surface of AlGa_N/Ga_N high electron mobility transistor based sensors

A. OULD-ABBAS^a, O. ZEGGAI^a, M. BOUCHAOUR^a, H. ZEGGAI^a, N. SAHOUANE^a, M. MADANI^a,
D. TRARI^a, M. BOUKAIS^a, N.-E. CHABANE-SARI^a

^aResearch unit of Materials and Renewable energies (URMER), University Abou Bakr Belkaïd, B.P. 119, Tlemcen, Algeria

A promising sensing technology utilizes AlGa_N/Ga_N high electron mobility transistors (HEMTs). HEMT structures have been developed for use in microwave power amplifiers due to their high two dimensional electron gas (2DEG) mobility and saturation velocity. The conducting 2DEG channel of AlGa_N/Ga_N HEMTs is very close to the surface and extremely sensitive to adsorption of analytes. HEMT sensors can be used for detecting gases, ions, pH values, proteins, and DNA. In this paper we review recent progress on functionalizing the surface of HEMTs for specific detection of glucose, kidney marker injury molecules, prostate cancer, and other common substances of interest in the biomedical field

(Received September 28, 2013; accepted November 7, 2013)

Keywords: HEMT, Semiconductor III-N, AlGa_N/Ga_N heterostructures, DNA, Sensor, 2DEG

1. Introduction

AlGa_N/Ga_N high electron mobility transistors (HEMTs) have shown great promise for broad-band wireless communication systems and advanced radar [1–2]. More recently these same structures have demonstrated the ability to perform as combustion gas sensors, strain sensors and also chemical, biological detectors [3–4]. In most cases, the application of some external change in surface conditions changes the piezoelectric-induced carrier density in the channel of the HEMT, have shown the strong sensitivity of AlGa_N/Ga_N heterostructures to ions, polar liquids, hydrogen gas, glucose, kidney marker injury molecules, prostate cancer, and other common substances. In particular they have shown that it is possible to distinguish these different analytes (biological substances).

The strong polarization discontinuity at the AlGa_N/Ga_N interface results in a positive polarization charge. This interface charge effect is compensated by a two-dimensional electron gas (2DEG) located at the Ga_N side, thus, forming the conductive channel of a high-electron-mobility transistor (HEMT) [5–6]. The 2DEG density is modulated by changes in the surface potential of the HEMT and thus, devices without gate metallization directly sense charged particles and molecules adsorbed onto the exposed gate area [7–8]. For these reasons AlGa_N/Ga_N HEMT devices are subject of intense investigation and have emerged as attractive candidates for pH and ion sensitive sensors or detectors for biological processes [9–10]. In this work, we investigate the different technological steps for sensor fabrication to various biological substances.

2. Description of the AlGa_N/Ga_N HEMT

High Electron Mobility Transistor (HEMT) also known as Two-dimensional Electron Gas Field Effect Transistor (TEGFET) is Schottky gate heterojunction transistor whose basic structure is described in Fig. 1. The semiconductor bandgap difference between Ga_N and its ternary alloy AlGa_N causes the apparition of a gas called two-dimensional electron gas (2DEG) composed of free charges confined in a quantum well at the interface. The charge accumulation is made possible by the action of the spontaneous polarisation whose orientation is highly dependent on the deposition process [11]. The 2DEG acts as a transistor channel with high mobility carriers, ideal for high frequency power applications

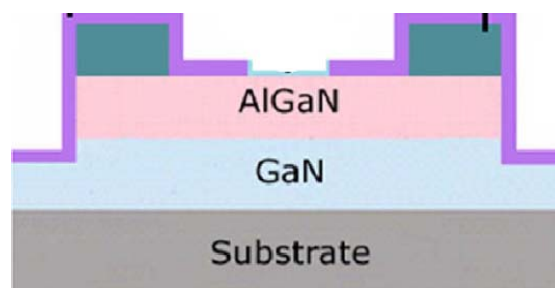


Fig. 1. schematic of HEMT.

The conducting (2DEG) channel of Ga_N/ AlGa_N based HEMTs is very close to the surface and its density changes under applied stress through piezoelectric polarization. This makes the device extremely sensitive to the ambient, which enhances detection sensitivity.

3. Biosensor fabrication

The HEMT structures typically consist of a 3 μm thick undoped GaN buffer, 30 \AA thick $\text{Al}_{0.3}\text{Ga}_{0.7}\text{N}$ spacer, and a 220 \AA thick Si-doped $\text{Al}_{0.3}\text{Ga}_{0.7}\text{N}$ cap layer. The epilayers are grown on thick GaN buffers on sapphire substrates. The gate area of HEMT is functionalized with different chemicals depending on the sensing applications [12].

Table 1 shows a summary of the surface functionalization layers we have employed for HEMT sensors to date. There are many additional options for detection of biotoxins and biological molecules of interest by use of different protein or antibody layers. The advantage of the biofet approach is that large arrays of HEMTs can be produced on a single chip and functionalized with different layers to allow for detection of a broad range of chemicals or gases [13].

Table 1. Summary of the surface functionalization.

Detection	Mechanism	Surface functionalization
H ₂	Catalytic dissociation	Pd, Pt
Pressure change	Polarization	Polyvinylidene fluoride
Botulinum toxin	Antibody	Thioglycolic acid/antibody
Proteins	Conjugation/hybridization	Aminopropylsilane
pH	Adsorption of polar molecules	Sc ₂ O ₃ , ZnO
KIM-1	Antibody	KIM-1 antibody
Glucose	GO _x immobilization	ZnO nanorods
Prostate-specific antigen	PSA antibody	Carboxylate succinyl ester/PSA antibody
Lactic acid	LO _x immobilization	ZnO nanorods
Chloride ions	Anodization	Ag/AgCl electrodes; InN
Breast cancer	Antibody	Thioglycolic acid/c-erbB antibody
CO ₂	Absorption of water/charge	Polyethyleneimine/starch
DNA	Hybridization	3-Thiol-modified oligonucleotides
O ₂	Oxidation	InGaZnO
Hg ²⁺	Chelation	Thioglycolic acid/Au

4. Examples of biodetection

4.1. Deoxyribonucleic acid (DNA) detection

The detection of deoxyribonucleic acid (DNA) oligomer hybridization to form duplex DNA using one immobilized strand on a surface is used in gene sequencing and diagnosis of genetic diseases.[14–15]

Existing methods to detect hybridization measure changes in the mass or optical and electrochemical properties and require prelabeling of the DNA target, special isotopes, fluorescence tags, or redox indicators [16–17].

Electrical detection of hybridization using semiconductor-based FETs have been reported previously.[18–19] Bauret al.[19] detected DNA hybridization on a functionalized GaN surface with fluorescence labeled DNA. It is generally considered that tethering DNA to Au films on the gate region of a FET provides a more reproducible result than using the native oxide on the GaN surface. The nature of interactions between gold surfaces and DNA are well established and are used to analyze duplex DNA sequences [20].

Fig. 2 shows a schematic cross section of the device with simple DNAs on the gold gate region and a photomicrograph of a completed sensor. The source-drain current-voltage characteristics were measured with the Au-gated region exposed to different DNA solutions. Three synthesized label-free 15-mer oligonucleotides (Sigma Genesys, St. Louis) were prepared to test DNA hybridization. Oligonucleotide probes, functionalized at the 3', ended with thiol group, and connected by a trimethylene linker, were prepared. The base sequence of this probe was 5'-AGATGATGAGAAGAA-3'-(CH₂)₃-thiol and the complementary target was 5'-TTCTCTCATCATCT-3'. To test the immobilization of 3 thiol-modified ss-DNA on the surface of the HEMT, the Au-gated area of the fabricated HEMT was exposed to buffered solutions, followed by exposure to thiol-modified DNA (~100 s), and then target DNA (~200 s). Hybridization between probe DNA and matched or mismatched target DNA on the Au-gated HEMT was detected. The HEMT drain source current showed a clear decrease of 115 μA as this matched target DNA was introduced to the probe DNA on the surface Fig. 3. Totally mismatched DNA was also used as a control and showed that nonspecific binding was absent [21-20-22].

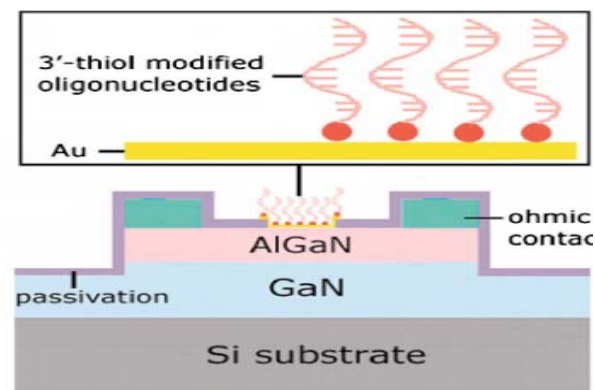


Fig. 2. Schematic of AlGaN/GaN HEMT with Au-coated gate area functionalized with 15-mer 3'-thiol-modified oligonucleotides.

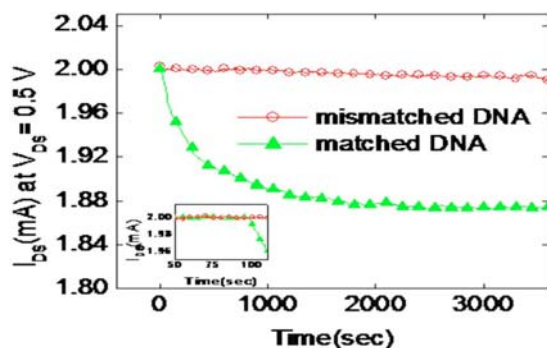


Fig. 3. Change in HEMT drain-source current at $V_{DS}=0.5$ V as a result of hybridization between immobilized thiol-modified DNA and matched or mismatched target DNAs [21].

4.2. Breast cancer

There is recent evidence to suggest that salivary testing for makers of breast cancer may be used in conjunction with mammography [23-24-25-26-27-28]. Saliva-based diagnostics for the protein c-erbB-2, have tremendous prognostic potential [29-30]. Soluble fragments of the c-erbB-2 oncoprotein and the cancer antigen 15-3 were found to be significantly higher in the saliva of women who had breast cancer than in those patients with benign tumors [31]. Other studies have shown that epidermal growth factor (EGF) is a promising marker in saliva for breast cancer detection [30-32]. These initial studies indicate that the saliva test is both sensitive and reliable and can be potentially useful in initial detection and follow-up screening for breast cancer. However, to fully realize the potential of salivary biomarkers, technologies are needed that will enable facile, sensitive, specific detection of breast cancer.

Antibody-functionalized Au-gated AlGaIn/GaN high electron mobility transistors (HEMTs) show promise for detecting c-erbB-2 antigen. The c-erbB-2 antigen was specifically recognized through c-erbB-2 antibody, anchored to the gate area. We investigated a range of clinically relevant concentrations from 16.7 $\mu\text{g/ml}$ to 0.25 $\mu\text{g/ml}$.

The Au surface was functionalized with a specific bifunctional molecule, thioglycolic acid. We anchored a self-assembled monolayer of thioglycolic acid, HSCH₂COOH, an organic compound and containing both a thiol (mercaptan) and a carboxylic acid functional group, on the Au surface in the gate area through strong interaction between gold and the thiol-group of the thioglycolic acid. The devices were first placed in the ozone/UV chamber and then submerged in 1 mM aqueous solution of thioglycolic acid at room temperature. This resulted in binding of the thioglycolic acid to the Au surface in the gate area with the COOH groups available for further chemical linking of other functional groups. The device was incubated in a phosphate-buffered saline (PBS) solution of 500 $\mu\text{g/ml}$ c-erbB-2 monoclonal antibody for 18 h before real time measurement of c-erbB-2 antigen.

After incubation with a PBS buffered solution containing c-erbB-2 antibody at a concentration of 1 $\mu\text{g/ml}$, the device surface was thoroughly rinsed off with deionized water and dried by a nitrogen blower. The source and drain current from the HEMT were measured before and after the sensor was exposed to 0.25 $\mu\text{g/ml}$ of c-erbB-2 antigen at a constant drain bias voltage of 500 mV. Any slight changes in the ambient of the HEMT affect the surface charges on the AlGaIn/GaN. These changes in the surface charge are transduced into a change in the concentration of the 2DEG in the AlGaIn/GaN HEMTs, leading to the slight decrease in the conductance for the device after exposure to c-erbB-2 antigen.

Fig. 4 shows real time c-erbB-2 antigen detection in PBS buffer solution using the source and drain current change with constant bias of 500 mV. No current change can be seen with the addition of buffer solution around 50 s, showing the specificity and stability of the device. In clear contrast, the current change showed a rapid response in less than 5 s when target 0.25 $\mu\text{g/ml}$ c-erbB-2 antigen was added to the surface. The abrupt current change due to the exposure of c-erbB-2 antigen in a buffer solution was stabilized after the c-erbB-2 antigen thoroughly diffused into the buffer solution. Three different concentrations (from 0.25 $\mu\text{g/ml}$ to 16.7 $\mu\text{g/ml}$) of the exposed target c-erbB-2 antigen in a buffer solution were detected. The experiment at each concentration was repeated five times to calculate the standard deviation of source-drain current response. The limit of detection of this device was 0.25 $\mu\text{g/ml}$ c-erbB-2 antigen in PBS buffer solution.

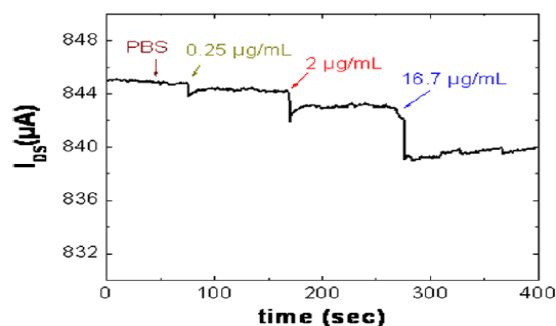


Fig. 4. Drain current of an AlGaIn/GaN HEMT over time for c-erbB-2 antigen from 0.25 $\mu\text{g/ml}$ to 17 $\mu\text{g/ml}$ [13].

4.3. Biotoxinsensors

The objective of this application is to develop and test a technology for detecting logical toxins. To achieve this objective, we have developed high electron mobility transistors (HEMTs) that have been demonstrated to exhibit some of the highest sensitivities for biological agents. Specific antibodies targeting Enterotoxin type B (Category B, NIAID), Botulinum toxin (Category A, NIAID) and ricin (Category B, NIAID), or peptide substrates for testing the toxin's enzymatic activity, have been conjugated to the HEMT surface. While testing still needs to be performed in the presence of cross-contaminants in biologically relevant samples, the initial

results are very promising. A significant issue is the absence of a definite diagnostic method and the difficulty in differential diagnosis from other pathogens that would slow the response in case of a terror attack. Our aim is to develop reliable, inexpensive, highly sensitive, with response times on the order of a few seconds, which can be used in the field for detecting biological toxins. This is significant because it would greatly improve our effectiveness in responding to terrorist attacks.

4.3.1. Botulinum

Antibody-functionalized Au-gated AlGaIn/GaN high electron mobility transistors (HEMTs) show great sensitivity for detecting botulinum toxin. The botulinum toxin was specifically recognized through botulinum antibody, anchored to the gate area. We investigated a range of concentrations from 0.1 ng/ml to 100 ng/ml.

The source and drain current from the HEMT were measured before and after the sensor was exposed to 100 ng/ml of botulinum toxin at a constant drain bias voltage of 500 mV, as shown in Fig. 5. Any slight changes in the ambient of the HEMT affect the surface charges on the AlGaIn/GaN. These changes in the surface charge are transduced into a change in the concentration of the 2DEG in the AlGaIn/GaN HEMTs, leading to the decrease in the conductance for the device after exposure to botulinum toxin.

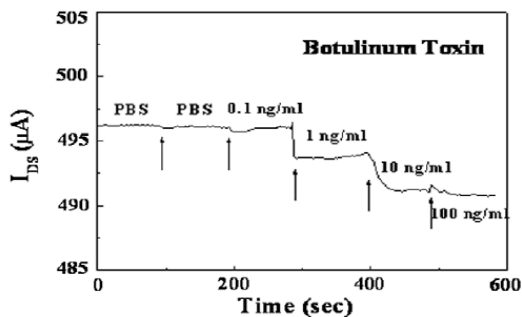


Fig. 5. Drain current of an AlGaIn/GaN HEMT versus time for botulinum toxin from 0.1 ng/ml to 100 ng/ml [13].

Fig. 5 shows a real time botulinum toxin detection in PBS buffer solution using the source and drain current change with constant bias of 500 mV. No current change can be seen with the addition of buffer solution around 100 s, showing the specificity and stability of the device. In clear contrast, the current change showed a rapid response in less than 5 s when target 1 ng/ml botulinum toxin was added to the surface. The abrupt current change due to the exposure of botulinum toxin in a buffer solution was stabilized after the botulinum toxin thoroughly diffused into the buffer solution. Different concentrations (from 0.1 ng/ml to 100 ng/ml) of the exposed target botulinum toxin in a buffer solution were detected. The sensor saturates above 10 ng/ml of the toxin. The experiment at each

concentration was repeated four times to calculate the standard deviation of source-drain current response. The limit of detection of this device was below 1 ng/ml of botulinum toxin in PBS buffer solution [13].

5. Conclusion

We have summarized recent progress in AlGaIn/GaN HEMT sensors. These devices can take advantage of the advantages of microelectronics, including high sensitivity, possibility of high-density integration, and mass manufacturability. The goal is to realize real-time, and inexpensive

There is great promise for using AlGaIn/GaN HEMT based sensors. Depending on the immobilized material, HEMT-based sensors can be used for sensing different materials. These electronic detection approaches with rapid response and good repeatability show potential for the investigation of airway pathology. The high surface area (gate) provides an ideal approach for enzymatic detection of biochemically important substances.

References

- [1] V. Tilak, B. Green, V. Kaper, H. Kim, T. Prunty, J. Smart, et al. *IEEE Electron Dev. Lett.* **22**(11), 504 (2001).
- [2] B. Luo, J. W. Johnson, J. Kim, R. M. Mehandru, F. Ren, B. P. Gila, et al. *Appl. Phys. Lett.* **80**, 1661 (2002).
- [3] O. Ambacher, M. Eickhoff, G. Steinhoff, M. Hermann, L. Gorgens, V. Werss, et al. *Proc ECS*, **214**, 27 (2002).
- [4] M. Stutzmann, G. Steinhoff, M. Eickhoff, O. Ambacher, C. E. Nobel, J. Schalwig, et al. *Diamond Rel Mater.* **11**, 886 (2002).
- [5] O. Ambacher, J. Smart, J. R. Shealy, N. G. Weimann, K. Chu, M. Murphy, W. J. Schaff, L. F. Eastman, R. Dimitrov, L. Wittmer, M. Stutzmann, W. Rieger, J. Hilsenbeck, *J. Appl. Phys.* **85**, 3222 (1999).
- [6] O. Ambacher, M. Eickhoff, A. Link, M. Hermann, M. Stutzmann, F. Bernardini, V. Fiorentini, Y. Smorchkova, J. Speck, U. Mishra, W. Schaff, V. Tilak, L. F. Eastman, *Phys. Stat. Sol. (c)* **0**, 1878 (2003).
- [7] R. Neuberger, G. Müller, O. Ambacher, M. Stutzmann, *Phys. Stat. Sol. (a)* **185**, 85 (2001).
- [8] M. Bayer, C. Uhl, P. Vogl, *J. Appl. Phys.* **97**, 033703 (2005).
- [9] B. S. Kang, F. Ren, L. Wang, C. Lofton, W. Tan Weihong, S. J. Pearton, A. Dabiran, A. Osinsky, P. P. Chow, *Appl. Phys. Lett.* **87**, 023508 (2005).
- [10] Y. Alifragis, A. Georgakilas, G. Konstantinidis, E. Iliopoulos, A. Kostopoulos, N. A. Chaniotakis, *Appl. Phys. Lett.* **87**, 253507 (2005).

- [11] F. Bernardini, V. Fiorentini, D. Vanderbilt, *Phys. Rev. B* **56**(16), R10024 (1997).
- [12] B. S. Kang, H. T. Wang, F. Ren, S. J. Pearton, *J. Appl. Phys.* **104**, 031101 (2008).
- [13] S. J. Pearton, F. Ren, Yu-Lin Wang, B. H. Chu, K. H. Chen, C. Y. Chang, Wantae Lim, Jenshan Lin, D. P. Norton, *Materials Science* **55**, 1 (2010).
- [14] I. J. Tinoco, *J. Phys. Chem.* **100**, 13311 (1996).
- [15] D.-S. Kim, H.-J. Park, H.-M. Jung, J.-K. Shin, P. Choi, J.-H. Lee, G. Lim, *Jpn. J. Appl. Phys., Part 1*, **43**, 3855 (2004).
- [16] H. Su, K. M. R. Kallury, M. Thompson, A. Roach, *Anal. Chem.* **66**, 769 (1994).
- [17] D. I. Han, D. S. Kim, J. E. Park, J. K. Shin, S. H. Kong, P. C. Choi, J. H. Lee, G. Lim, *Jpn. J. Appl. Phys., Part 1*, **44**, 5496 (2005).
- [18] T. Ohtake, C. Hamai, T. Uno, H. Tabata, T. Kawai, *Jpn. J. Appl. Phys., Part 2*, **43**, L1137 (2004).
- [19] B. Baur, G. Steinhoff, J. Hernando, O. Purruicker, M. Tanaka, B. Nickel, M. Stutzman, M. Eickhoff, *Appl. Phys. Lett.* **87**, 263901 (2005).
- [20] M. A. Garcia, S. D. Wolter, T. H. Kim, S. Choi, M. Losurdo, G. Bruno, *Appl. Phys. Lett.* **88**, 013506 (2006).
- [21] B. S. Kang, S. J. Pearton, J. J. Chen, F. Ren, J. W. Johnson, R. J. Therrien, P. Rajagopal, J. C. Roberts, E. L. Piner, K. J. Linthicum, *Appl. Phys. Lett.* **89**, 122102 (2006).
- [22] D. Y. Petrovykh, H. Kimura-Suda, L. J. Whiteman, M. J. Tarlov, *J. Am. Chem. Soc.* **125**, 5219 (2003).
- [23] J. S. Michaelson, E. Halpern, D. B. Kopans *Radiology*, **212**(2), 551 (1999).
- [24] T. Harrison, L. Bigler, M. Tucci, L. Pratt, F. Malamud, J. T. Thigpen, et al. *Spec Care Dent* **18**(3), 109 (1998).
- [25] C. Streckfus, L. Bigler, T. Dellinger, M. Pfeifer, A. Rose, J. T. Thigpen, *Clin Oral Invest.* **3**(3), 138 (1999).
- [26] C. Streckfus, L. Bigler, T. Dellinger, X. Dai, W. J. Cox, A. McArthur, et al. *Oral Surg Oral Med Oral Pathol Oral Radiol Endod.* **91**(2), 174 (2001).
- [27] R. McIntyre, L. Bigler, T. Dellinger, M. Pfeifer, T. Mannery, C. Streckfus, *Oral Surg Oral Med Oral Pathol Oral Radiol Endod.* **88**(6), 687 (1999).
- [28] C. F. Streckfus, L. R. Bigler, M. Zwick, *J Oral Pathol Med.* **35**(5), 292 (2006).
- [29] L. R. Bigler, C. F. Streckfus, L. Copeland, R. Burns, X. Dai, M. Kuhn, et al. *J Oral Pathol Med* **31**(7), 421 (2002).
- [30] W. R. Chase, *J Mich Dent Assoc.* **82**(2), 12 (2000).
- [31] C. Streckfus, L. Bigler, *Adv Dent Res.* **18**(1), 17 (2005).
- [32] S. Z. Paige, C. F. Streckfus, *Gen Dent.* **55**(2), 156 (2007).

*Corresponding author: aouldabbes@yahoo.fr